Mansoura Engineering Journal

Volume 49 | Issue 4 Article 4

2024

Influence of macro-synthetic fibers on the flexural behavior of high strength concrete beams reinforced with GFRP bars

Maryam M. Koura
Researcher, Structural Engineering Department, Faculty of Engineering, Mansoura University, Mansoura, Egypt, maryamkoura8@gmail.com

Ahmed M. Tahwia
Professor at Structural Engineering Department, Faculty of Engineering, Mansoura University, Mansoura, Egypt

Mohamed H. Matthana
Associate Professor in the Department of Structural Engineering, Faculty of Engineering, Mansoura University, Mansoura, Egypt

ORIGINAL STUDY

Influence of Macro-synthetic Fibers on the Flexural Behavior of High Strength Concrete Beams Reinforced with GFRP Bars

Maryam M. Koura*, Ahmed M. Tahwia, Mohamed H. Matthana

Structural Engineering Department, Faculty of Engineering, Mansoura University, Mansoura, Egypt

Abstract

Rusting of steel reinforcement in marine environments causes the overall destruction of reinforced concrete constructions; steel rebars in concrete members have been replaced with fiber-reinforced polymer (FRP) bars in recent years. To enhance the shear behavior of glass (GFRP) bars reinforced concrete (RC), macro-synthetic polyolefin (PO) fiber was added. These materials have a low modulus of elasticity, a high tensile strength, and a linear stress—strain response to full failure. This study investigates the effect of macro synthetic structural fibers on the post-cracking and deformability properties of high strength concrete reinforced with FRP bars without transverse reinforcement. Eight full-scale RC beams (without stirrups) are subjected to a two-point loading system by varying the presence of PO fiber and evaluated under flexural. The test specimens include (i) four beam GFRP reinforcement, one control beam without macro fiber and three beams with different PO fiber ratios (0.28%,0.44%,0.60%) (ii) four beam steel reinforcement, one control beam without macro fiber and three beams with different PO fiber ratio (0.28%,0.44%,0.60%) all beams have reinforcement ratio 0.4%. The addition of fiber to the concrete mix reduced slightly compressive strength by 5%, while the split tensile strength was greatly enhanced by 19%, the post-cracking action and flexural behavior increased by increasing the ductility level by 18.3%, according to the experimental results. Furthermore, as fiber dosage increased, crack widths at service loads decreased significantly and improved the deformability of GFRP and steel-reinforced concrete beams.

Keywords: Macro synthetic fiber, High strength concrete, GFRP bars, Beams, Load carrying capacity

1. Introduction

Recently, a Fiber-reinforced polymer (FRP) bar is regarded to be a promising substitute for traditional reinforcing steel bars in concrete reinforcement, relatively a new technique. In terms of conventional steel's inherent corrosion nature, FRP rebars are ideal for reinforcing concrete elements in harsh environments and can improve the durability of concrete structures (Li et al., 2022; Zhu et al., 2018; Imam et al., 2021). Dashti and Nematzadeh (2020) investigated the effects of Forta-Ferro (FF) fiber and calcium aluminate cement (CAC) on the flexural behavior of concrete beams reinforced with glass fiber-reinforced polymer (GFRP) rebars subjected to acid attack and found that the optimum content of FF fibers for improving the mechanical properties of concrete, as well as the flexural behavior of beams, is 0.4%. Further, using 0.7% FF fibers proved to be very effective in controlling the mechanical strength reduction of concrete and the flexural strength of beams immersed in acid (Dashti and Nematzadeh, 2020). Due to the nonmagnetic and noncorrosive nature of FRP materials, they can be used to avoid electromagnetic interference and steel corrosion. Furthermore, FRP bars also have the benefits of high tensile strength, rigidity, and low weight when compared to steel rebar, making it simple to handle and reducing application time and overall cost (Liu et al., 2019). However, using FRP bars remains a tough task for engineers because of the significant variations between FRP and traditional steel in

Received 31 January 2024; revised 5 March 2024; accepted 14 March 2024.
Available online 24 April 2024

* Corresponding author.
E-mail address: maryamkoura8@gmail.com (M.M. Koura).

https://doi.org/10.58491/2735-4202.3205

terms of physical and mechanical properties. FRP bars have a much lower elastic modulus than steel bars. According to the literature, the most utilized classes of customized FRP rebars are glass fiber-reinforced polymer (GFRP) and carbon fiber-reinforced polymer (CFRP). In this research study GFRP bars. The modulus of elasticity of glass fiber-reinforced polymer (GFRP) bars varies from 35 to 50 GPa. This FRP bar-reinforced concrete beam with low elastic modulus exhibits increased deflection and crack breadth when compared to steel-reinforced concrete beams with the same reinforcement ratio (Joshi et al., 2018; Issa et al., 2011). To solve deformability constraints, ductility and crack width of FRP-bar-reinforced concrete beams, a distinct strategy utilizing concrete reinforced with macro-synthetic polyolefin fiber.

Higher grades of concrete strength have resulted from advancements in material technology and production. There has been a noticeable global trend in using high-strength concrete (compressive strength, $F_{cu} > 50$ MPa) in building projects in recent years. When considering structural engineering attributes, high-strength concrete (HSC) outperforms traditional normal-strength concrete (NSC) by offering much better values regarding stiffness, economy, durability, and compressive and tensile strengths. The strength of concrete increases by lowering the water-to-cement ratio and adding silica fumes (Tahwia et al., 2022; Tahwia et al., 2023a).

The load-carrying capability of beams reinforced with FRP bars is greater than that of beams reinforced with steel bars of equal area. Usually, FRP-reinforced concrete beams' failure results in brittle behavior due to fiber rupture (Sheikh and Kharal, 2018; Abdelkarim et al., 2019). The review of the literature has shown that the efficiency of beams with FRP bars can increase by incorporating discrete fibers into concrete, which can also produce pseudo-ductility (Yoo et al., 2016a). Yang et al. (Yang et al., 2012; Pereira et al., 2012) investigated the impact of steel and synthetic fibers addition on the performance of RC members reinforced with FRP bars under flexural loads. The effects of fiber addition on ductility, cracking resistance, and load-carrying capacity were investigated. They conclude that the FRP bar-reinforced concrete beams' ductility, ultimate flexural strength, and first-cracking load all increased with adding fibers. While also mitigating the large crack width. Wang and Belarbi (2011) examined the viability of combining polypropylene fiber-reinforced concrete and FRP reinforcement to create a hybrid steel-free reinforcement solution for concrete beams and described the crack width and deformability of 12 beams under flexural and reference FRP/plain concrete beams of this FRP/FRC hybrid reinforcing system. They improved FRP-reinforced beams' deformability by using micro polypropylene (nonstructural) fibers with a constant volume proportion of fibers of 0.5%. According to test results, FRP/FRC beams have fewer crack widths than FRP/plain concrete beams. In contrast to a similar beam, the inclusion of fibers improved flexural behavior by more than 30% through increasing ductility. Ge et al. (2015) researched the flexural properties of hybrid concrete beams reinforced with steel and basalt fiber-reinforced plastic (BFRP) bars are examined. The result shows that BFRP bars' tensile destruction is more abrupt than steel bars because they have a higher tensile strength but a lower elastic modulus. The BFRP bars showed a mechanical failure mechanism as FRP polymers take the brittle failure mode if it reaches its ultimate capacity (Erfan et al., 2019; El-Sayed et al., 2023). Many studies have shown that adding steel fibers to over-reinforced steel reinforced beams and high-strength steel reinforced beams increases their ductility. However, only some studies relating to the behavior of concrete beams reinforced with FRP bars and the influence of fibers have been conducted. Additionally, prior research has solely concentrated on using steel or tiny

Nomenclature

PO	Macro-synthetic polyolefin
ρ_{FRP}	Ratio of FRP reinforcement
ρ_S	Ratio of steel reinforcement
V_f	Fiber volume fraction
A_{FRP}	Area of the cross-section of FRP bars (mm^2)
A_S	Area of the cross-section of steel bars (mm^2)
F	Fracture load (N)
b	Beam width (mm)
d	Effective depth of the section (mm)
Mp	Peak moment (kN.m)
Δ	Deflection of mid-span (mm)
P	Applied load (kN)
S	The test specimen's shear span (mm)
E_c	Concrete's modulus of elasticity (MPa)
Es	Steel bar modulus of elasticity (MPa)
I_e	Effective moment of inertia (mm^4)
L	Length of the beam (mm)
I_g	Gross inertia moment (mm^4)
h	Height of the beam (mm)
I_{cr}	Cracked moment of inertia (mm^4)
k	Bond dependent coefficient
n_f	The modular ratio of FRP reinforcement and concrete
Mcr	Moment of cracking (kN.m)
M_a	Peak moment (kN.m)
α	Effective coefficient of fibers
γ	Factor that is affected by boundary conditions and loads

synthetic fibers to create ductile behavior. The usage of macro-structural synthetic fibers has become more popular in recent years due to their enhanced qualities, such as resistance to corrosion and flexibility, which can help mitigate some of the drawbacks of steel fibers. The results in this paper provide important experimental information on synthetic fiber reinforced GFRP beams with no stirrups and enhanced shear behavior (Tran et al., 2020; Erfan et al., 2021) that currently need to be added to the existing literature. The use of GFRP reinforcement bars instead of steel bars had a slight effect on increasing the failure loads of the beams for the same compressive strength (El-Sayed et al., 2022; El-Sayed and Algash, 2021; Nassif et al., 2021). The steel fibers play a great role in resisting the shear stresses of UHPFRC deep beams (Yousef et al., 2018; Al-Enezi et al., 2023; Yousef et al., 2023). According to the experimental results, it is well-known that steel fibers are used to enhance concrete shear capacity and post-cracking tensile strength since FRC is characterized by enhanced toughness due to the bridging effects provided by steel fibers (Susetyo et al., 2011). Steel fibers also provide substantial post-peak resistance, ductility and can transform brittle mode of failure into ductile ones (Ding et al., 2011; Ashour et al., 1992).

The novelty of this research is to evaluate the effect of structural macro-synthetic fibers on the flexural behavior of HSC beam reinforced with steel and GFRP bars without transverse reinforcement. A four-point bending test was conducted to assess flexural crack initiation, flexural crack propagation, the pattern of cracks at the ultimate stage, failure mode and failure load.

2. Research significance

New design techniques and fiber components have been intensively employed and researched to create an RC structure with no corrosion by using GFRP and synthetic macro-fibers to reinforce concrete beams. This hybrid system is projected to reduce deterioration caused by steel reinforcement while keeping the required strength and stiffness. The insertion of PO fibers can successfully stop structural cracks with RC components with low internal stiffness, like GFRP bars, and greatly improve deformability and post-peak behavior.

Hence, the research aims to study the flexural behavior of RC beams reinforced internally using GFRP bars. Also, study the impact of different ratios of PO fibers on the total performance improvement of GFRP beams under flexure, comparing results with the same steel-reinforced beam.

The aim of this research is to:

(a) Determine the impact of various PO fiber doses (0.28%,0.44%,0.60%) on the high strength concrete beams reinforced with GFRP bars subjected to flexure, evaluate the fracture reaction of synthetic fibers concerning for reducing crack width and deflection limitations and analyze the impact of fiber insertion on GFRP beams which enhance general load deformation and failure performance compared to steel RC beams.
(b) Study influence fiber doses of macro synthetic polypropylene fibers in concrete instead of traditional transverse shear stirrups on the behavior of research beams to accomplish the required failure mechanism and increased lateral load resistance participants of the RC.

3. Experimentation program

Eight full-scale test specimens of RC beams made of plain concrete and fiber-reinforced concrete (FRC) were exposed to an experimental investigation; four beams reinforced with steel, four reinforced with GFRP bars and three fiber dosage levels were considered. The length of each test sample was 1.90 m, having a rectangular cross-section of 150 mm × 250 mm (Table 1).

Test participants comprise (i) four beams reinforced with GFRP bars (ρ_{FRP} = 0.4%), one control

Table 1. Test matrix.

Sample ID	The fiber content (kg)	Bars' area (mm^2)	Reinforcement ratio ρt (%)	Longitudinal reinforcement type
GFRC 00	–	2Φ10 = 157	0.4	GFRP
GFRC 2.5	2.5	2Φ10 = 157	0.4	GFRP
GFRC 4.0	4.0	2Φ10 = 157	0.4	GFRP
GFRC 5.5	5.5	2Φ10 = 157	0.4	GFRP
RC 00	–	2Φ10 = 157	0.4	Steel
RC 2.5	2.5	2Φ10 = 157	0.4	Steel
RC 4.0	4.0	2Φ10 = 157	0.4	Steel
RC 5.5	5.5	2Φ10 = 157	0.4	Steel

Note: (a) 'GFRC' signifies beams with GFRP bars reinforcement; 'RC' signifies beams with steel bars reinforcement; (b) 00, 2.5, 4.0 and 5.5 signifies to the various fiber doses, which range from 0% to 0.6%.

beam with no fiber addition and three beams with fiber (0.28%,0.44%,0.60%). (ii) four beams with steel reinforced bars ($\rho_S = 0.4\%$), one control beam with no fiber addition, and three beams with fiber (0.28%,0.44%,0.60%).

The present study aims to investigate the influence of varied ratio additions of macro synthetic structure fiber on beam behavior with GFRP bars reinforced and contrast this with the same beams with steel bars reinforced. For all beams, the reinforcement ratio is 0.4% and were supposed to fail in reinforced configuration with fiber ratio 0.28%, 0.44%, and 0.6% to investigate flexural behavior on beams as shown in Fig. 1. The GFRP's elastic modulus ($E_{FRP} = 40$ GPa) is just 20%, in comparison to steel ($E_S = 210$ GPa). Furthermore, standard experiments on cylinders, cubes and small-scale beams were carried out to explore the impact of fiber content on the compressive, flexural strengths and splitting tensile on concrete.

3.1. Material characteristics

3.1.1. Concrete mixture

A concrete mixture with a cubic compressive strength of 60 MPa was created using the following material: 1- Portland cement type I (CEM-I 42.5 N). The cement product according to the Egyptian Standard ES 4576-1 (2022). Table 2 lists the cement's physical and mechanical characteristics as well as the Egyptian standard criteria, 2- coarse aggregate well graded locally crushed stone type 4/10 from the Suez Attakai quarry, 3- fine aggregate was natural sand from type 0/4, the physical parameters of fine and coarse aggregate are provided in Table 3, 4- silica-fume with specific surface area of 17 000 m^2/kg, 5- potable water was used, 6- chemical additives, superplasticizer type G according to ASTM C 494, 7- macro-synthetic fibers were produced by BASF Construction Chemicals. Following several trials, the concrete mix proportions in (kg/m^3) were

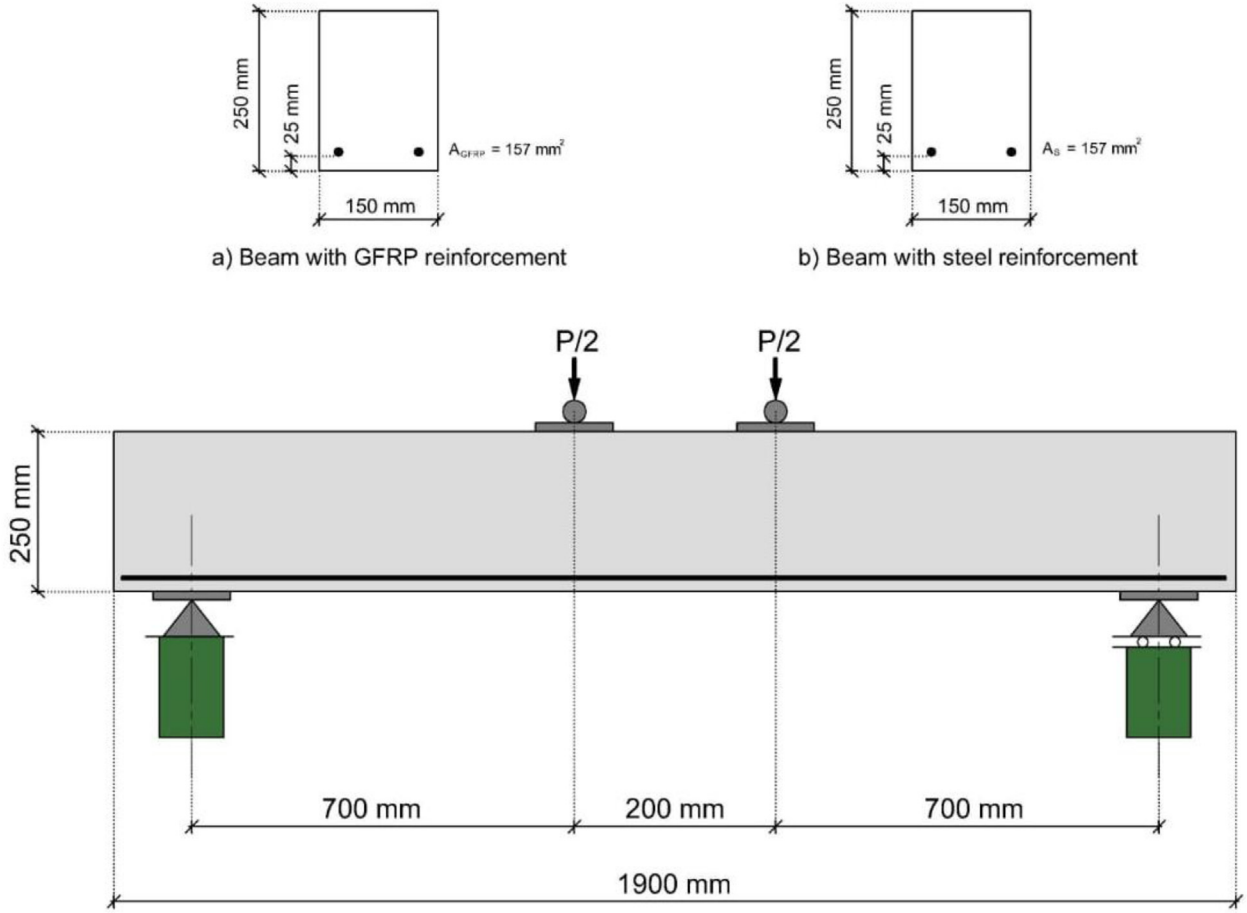

Fig. 1. Details of reinforcement and cross section of beams.

Table 2. Cement's physical and mechanical properties.

Property	Results	ES 4756–1:2022 limits
Soundness (mm)	1.0	≤10
Initial setting time (min)	155	≥60
Final setting time (min)	200	–
Compressive strength @ 2 days (MPa)	8.6	≥10
Compressive strength @ 28 days (MPa)	47.6	42.5 ≤ X ≤ 62.5

Table 3. Aggregate properties.

Property	Coarse aggregate	Fine Aggregate	Specifications
Fine particles (%)	0.4	0.9	≤2.5%
Water absorption (%)	1.78	0.81	≤2.5%
Specific gravity	2.64	2.62	–

determined in Table 4. In order to get adequate concrete mixing, The following were the different processes in the mixing of concrete: First, A saturated surface-dry state was achieved by thoroughly combining fine, coarse particles and cement mixed well, then adding 50% of the total water content. Finally, the superplasticizer was mixed with the remaining water and properly mixed up into a concrete mix. In the instance of FRC, fibers were progressively sprayed on top of the mixture to achieve a uniform and workable mix. The typical cylinders, cubes and small-scale prismatic beams were produced using concrete samples from each batch. Fig. 2 illustrates the concrete mix and how the test samples were prepared before, during, and after casting. To achieve a smooth application surface of the load, the top surfaces of the samples were extensively levelled and completed. Fig. 3 illustrates all samples for each mixture.

3.1.2. GFRP bars

Glass fiber reinforced plastic (GFRP) reinforcement bars are created by mixing glass fibers with polymers which can include epoxy, polyester resin, or vinyl ester. The incorporation of glass fibers and polymers results in extremely strong and long-lasting GFRP reinforcement bars; the glass fibers offer strength and durability, while the polymers offer flexibility and concrete adhesion. They are frequently used as an alternative to conventional steel reinforcement bars in concrete structures. In this study, longitudinal GFRP main reinforcements with a diameter of 10 mm from reinforced fiber industries company (Russian company Armastek) in Egypt. The characteristics of GFRP reinforcement are given in Table 5.

3.1.3. Structural macro-synthetic polypropylene fiber

The synthetic fibers and GFRP reinforcement employed in this investigation are depicted in Fig. 4.

Table 4. Concrete mix design for 1.0 cubic meter (kg).

No. of Mix	Type of mixture	Cement	Silica fume	Sand	Agg. 1	Water	SP	Fiber
M1	PC	450	50	680	1050	160	11.5	–
M2	FRC	450	50	680	1050	160	11.5	2.5
M3	FRC	450	50	680	1050	160	11.5	4
M4	FRC	450	50	680	1050	160	11.5	5.5

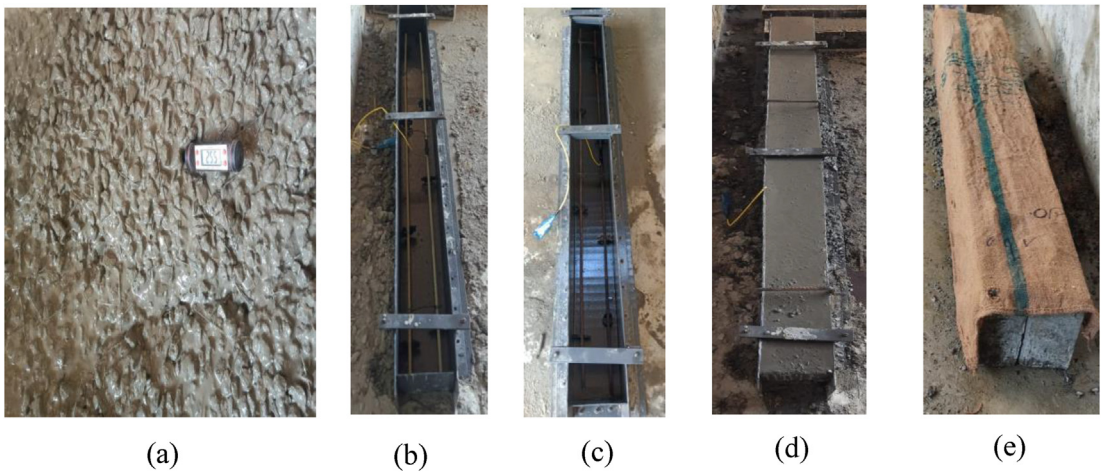

Fig. 2. Specimen preparation: (a) Fresh concrete and its temperature recording, (b) Fiber reinforcement form, (c) Steel reinforcement form, (d) Fully cast specimen, (e) Beams curing with wet burlap.

Fig. 3. All samples for each mixture.

Table 5. The mechanical characteristics of steel and GFRP reinforcement.

Material	Bar Diameter (mm)	Nominal area (mm2)	Yield strength (MPa)	Tensile strength (MPa)	Modulus of elasticity (GPa)	Elongation (%)
GFRP	10	78.57	–	1035	40	2.5
Steel	10	78.57	444	615	200	28

The properties of used macro synthetic polyolefin are given in Table 6.

3.2. Compressive, tensile strength and modulus of elasticity of concrete mix

The Compression strength of concrete was determined by a cube with standard dimensions 150 × 150 × 150 mm (Fig. 5 a) and tensile strength by cylinders size 150 mm × 300 mm (Fig. 5 b) for concrete mix with and without fiber according to the **EN 12390–3 standard** (BS EN 12390-3, 2009). At least three samples were examined from each mixture to describe the material characteristics of concrete. At 28 days of water curing, the average concrete strength, tensile strength and modulus of elasticity are presented in Table 7. Previous studies have demonstrated that the ultimate strain of concrete under compression and tension can be greatly increased by adding fiber up to a volume fraction of 1.0%. The failure mode changed from being more ductile flexure dominant to being less ductile

(a) (b)

Fig. 4. GFRP reinforcement and synthetic fiber are employed in RC beams.

Table 6. Mechanical and physical characteristics of macro-synthetic fiber.

Properties	Value
Material	polyolefin 100% (colorless)
Design	Monofilament
Specific gravity	0.91 g/cm^3
Equivalent diameter	0.85 mm
Length	48 mm
Aspect ratio (L/D)	56.5
Alkali resistance	Excellent
Tensile strength	400 MPa
Modulus of elasticity	4.7 GPa
Absorption	Nil
Melting point	160 °C
Ignition point	350 °C
Chemical resistance	Excellent

flexure-shear (Lakavath et al., 2019a; Tahwia et al., 2023b). As a result, the ultimate strain of concrete is increased, which increases the pseudo ductility of GFRP RC beams constructed to fail in compression-controlled conditions.

The splitting tensile strength was calculated as 2P/πDL, where P is the failure load, D and L are the cylinders' diameter and height as **ASTM C496 standard** (ASTM C496/C496M, 2017). In comparison to plain concrete, MF 5.5 containing 0.55% PO fibers showed the greatest increment of 50% in spitting tensile strength. In contrast, cylinders of plain concrete failed immediately because of the creation of one crack that extends vertically. The failure of other FRC cylinders, which contain PO fiber, was only simple vertical and horizontal cracking due to stress re-distribution along the failure plane as (Sahoo et al., 2015).

The modulus of elasticity is an essential mechanical parameter used to assess the behavior of concrete. According to the **ASTM C469 standard** (ASTM C469/C469M, 2014), the outcome of three tests of 150 mm × 300 mm cylindrical samples for PC and FRC mixtures at 28 days were averaged to determine the modulus of elasticity as shown in Fig. 5c. Concrete test specimens were condensed to approximately 40% of the maximum load for this test. Table 7 reports the modulus of elasticity for different mixtures.

In this research was noted that the inclusion of PO fiber with a volume fraction of 0.28–0.6% to the concrete mix slightly decreased the compressive strength gradually by 5% (Fig. 6a); all FRC cubes did not entirely crush due to the fibers' bridging performance but retained their reliability through the test's completion. On contrast, the indirect tensile strength of the specimens was increased by increasing ratio of PO fiber by 19% as shown in Fig. 6b.

3.3. Modulus of rupture of concrete specimens

The residual bending strength (f_R) of fiber-reinforced concrete specimens is a fundamental post-cracking parameter. The test for fracture was performed as **ASTM C293 standard** (ASTM C293/C293M, 2016) to determine how various macro synthetic fiber doses affect GFRP reinforced beams. A 100 × 100 × 500 mm concrete prism was used for the fracture study. Fig. 7 shows the three-point bending test set-up. The residual bending strengths

(a) (b) (c)

Fig. 5. Test setup for compression, splitting tensile, and modulus of elasticity tests.

Table 7. Concrete's tensile and compressive strength.

Mixture ID	Average compressive strength of cube (MPa)	Standard deviation (MPa)	Tensile strength (MPa)	Modulus of elasticity (GPa)
MF 00	67.9	1.28	6.45	38.6
MF 2.5	66.2	1.52	6.75	41.9
MF 4.0	65.1	1.47	7.05	40.5
MF 5.5	64.5	1.23	7.65	40.1

(f_R) were calculated using RILEM TC162 recommendations Eq. (1) (Buratti et al., 2011). The results of residual bending strength (f_R) for control and variable ratio of PO fiber reinforced specimens are clarified in Table 8 and Fig. 8. The control specimens failed in the bending test, despite other specimens with different PO fiber ratios having a simple linear crack. As a result, the macro-synthetic fibers greatly

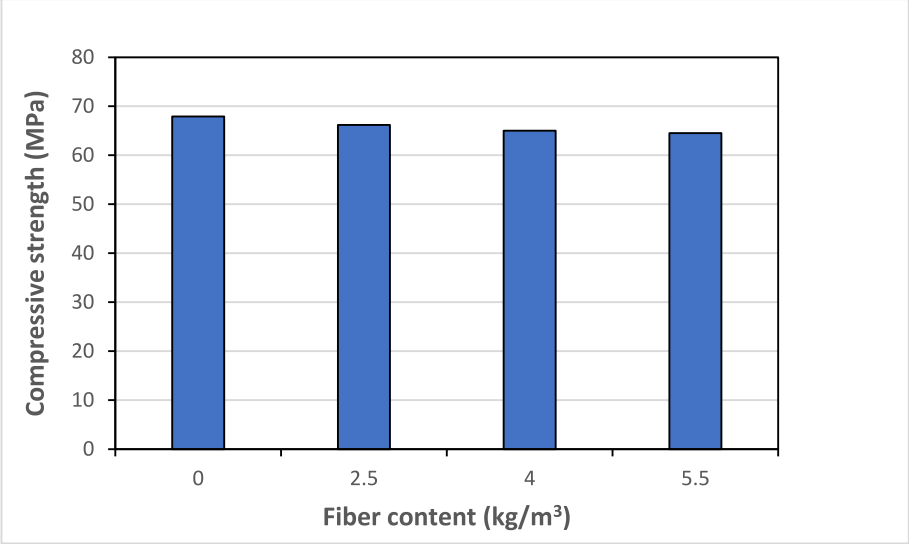

a- Compressive strength

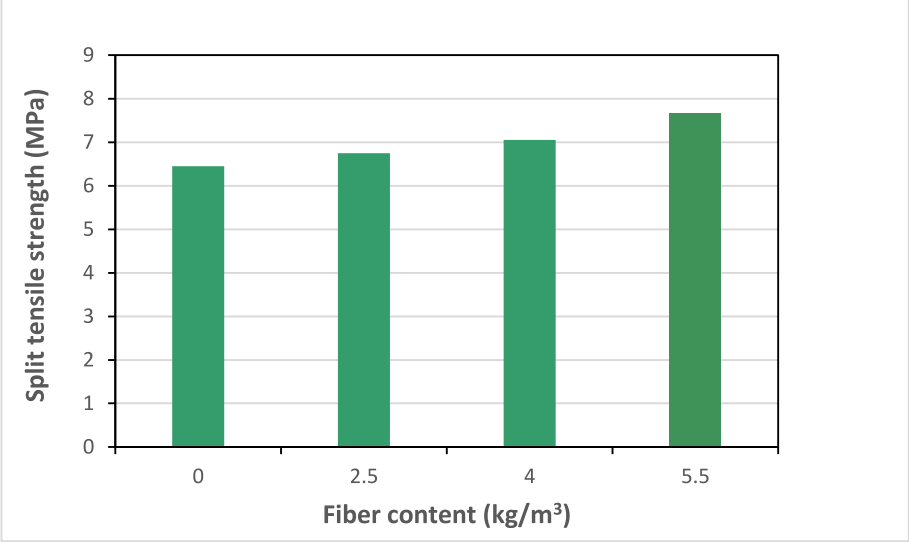

b- Tensile strength

Fig. 6. Compressive and tensile strengths test results at 28 days.

(a) Beam with PO fiber 00 (b) Beam with PO fiber 5.5

Fig. 7. Flexural test setup for beams with and without macro synthetic fiber.

Table 8. Results of flexural test.

Specimen ID	Average Fracture Load (kN)	flexural strength (MPa)
MF 00	11.5	8.6
MF 2.5	12	9
MF 4.0	12.5	9.4
MF 5.5	13.6	10.2

enhanced the post-cracking behavior, as demonstrated by the fracture tests. Increased fiber content led to an increase in post-cracking stiffness and fracture energy. The beam with no fiber exhibits a complete fracture, but other beams with varying PO fiber ratios have a simple crack, as shown in Fig. 7.

$$f_R = \frac{3FL}{2bd^2} \quad (1)$$

4. Test set-up

All of the beams underwent flexure testing and were simply supported by two rigid supports, subjected to a concentrated bending load at their mid-span that gradually increased until failure. Fig. 9 (a) shows a displacement-controlled profile. A hydraulically powered jack with a 1000 kN capacity was employed to apply the monotonic loading. The distance between the two loading beams measured 200 mm. The specimens were supported on both ends by rigid support with a 150 mm edge separation and a shear span of 700 mm. The vertical deflection and profile of curvature of the beams were measured in the middle of the span by using a dial gauge. The instrumentation specifications are shown in Fig. 9 (b). The beams were captured in high-resolution photos using a 64-megapixel camera with a 26 mm focal length lens. A strain gauge

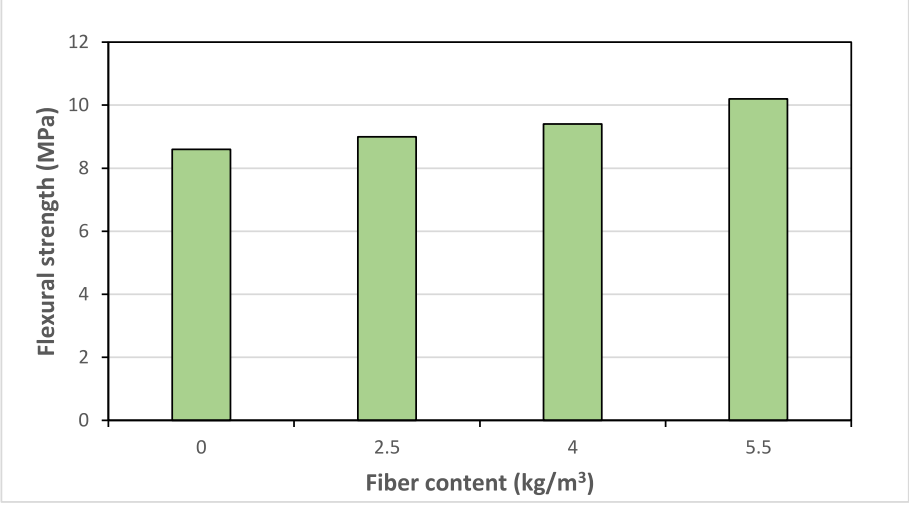

Fig. 8. Influence of fiber content on flexural strength of specimens.

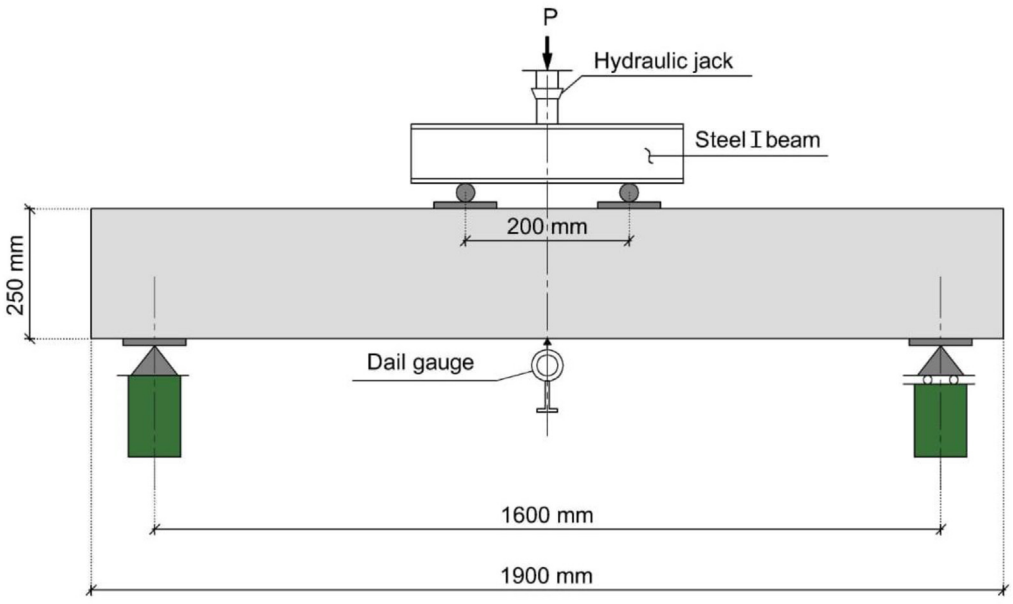

(a) Schematic test setup.

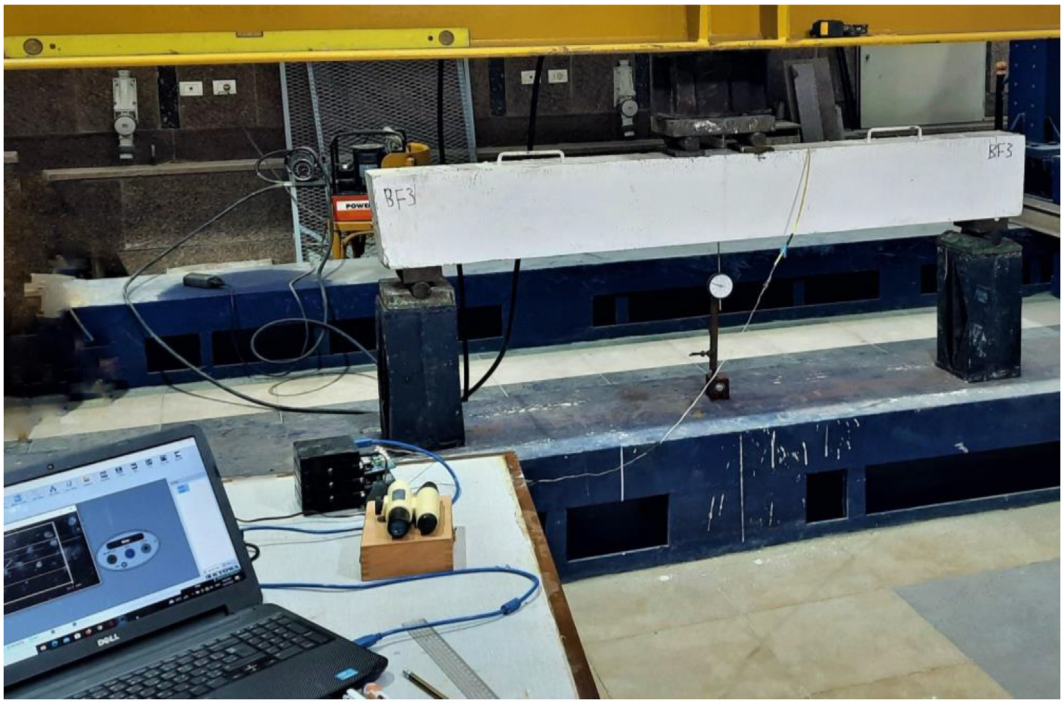

(b) Actual test setup

Fig. 9. Test setup and instrumentation.

was used to gauge the strain in GFRP bars, and an automatic data acquisition system (DAQ) was used to record the strain values at a frequency of 2 Hz that was used to link these sensors in real-time throughout the testing procedure (Lakavath et al., 2019b). The load was applied to the beams through a load-controlled mode with a loading rate of 10–20 kN/min.

5. Results and discussion

5.1. Load displacement curves

The analysis of each of the samples' experimental outcomes is provided in Table 9. To comprehend the impact of adding macro-synthetic fiber and the impact of the longitudinal GFRP ratio, all specimens' load–displacement curves are compared. The first cracking point was defined as the point at which the strain measured by the strain gauges rapidly rose in response to a slight change in load. The post-cracking stiffness is defined as the load–displacement curve slope following occurrence at the initial crack of flexural. Beam stiffness enhanced in steel reinforced over GFRP beams by 10 kN in cracking load. The service load is the point when utilization is 30% of peak capacity. The tested beams' ductility and deformation factor were determined using an energy-based technique (Oudah and El-Hacha, 2012; Yoo et al., 2016b).

5.1.1. Control beams with steel and GFRP reinforcement

All beams have the same low-tension reinforcement ratio (ρ_t = 0.4%). The control steel beam acquired a yield point at load 70 kN. The steel-reinforced beam's average peak load was discovered with a value of 118 kN and the sample was displaced by approximately 26.5 mm. The beam's post-cracking rigidity was calculated using the curve of load–displacement portion following the beginning of the first crack. The value of post-cracking rigidity for two control beams, Steel and GFRP reinforced with the same concrete mixture was 33 and 10 kN respectively Table 9. The control GFRP beam samples had a cracking load of 20 kN, yield point at load 55 kN and peak load of 64 kN comparable to a displacement of 11 mm. Considering all that was given steel reinforcement beam had a value of peak load higher than the GFRP reinforced beam by 50% due to the brittle fashion of FRP bars ruptures under tension without exhibiting deformability.

During GFRP, bars were substituted with the steel reinforcement of equivalent area 0.4%; the load of crack and post cracking rigidity of the beams (RC 00) were 30 kN and 33 N/mm, consequently. The capacity of peak load (RC 00) was determined to be 118 kN, which is 84% greater than GFRP reinforced sample (Fig. 10). The beams of steel reinforcement demonstrated increased load-carrying performance in comparison to GFRP beams. The GFRP reinforcement beam effectively stopped the spread of the flexural fracture in the constant moment zone but was unable to restrict the shear span from collapsing due to flexure shear.

5.1.2. GFRP beams with 0.28% fiber content

The incorporation of 0.28% fiber to GFRP-reinforced samples (GFRC 2.5) reduced the load reduction following the first crack in comparison to specimens without fiber addition (GFRC 00); the decrease in load after the first cracking decreased by 30 to 20 kN. Furthermore, when compared to (GFRC 00(specimens, the post cracking rigidity improved by 67% (6.7 kN/mm). The maximum carrying capability load 'peak load' of the specimens was 91 kN, wich was only 4.2% greater than the beams with no fiber (GFRC 00). In addition, the deformation factor didn't increase significantly. Beams without PO fiber experienced greater displacement and a larger crack opening shear failure despite the beam with 0.28% (GFRC 2.5) that had a flexure cracking at maximum load. As a result, the fibers' contributions at high displacement were high Which leads to an appreciable change in the deformation factors.

5.1.3. Steel reinforced beams using 0.28% fibers

Cracking load and post-cracking rigidity for (RC 2.5) beam was determined to be 40 kN and 37 kN/mm, consequently, in comparison to control specimens (RC 00). The insertion of fibers to the beams

Table 9. Analysis of test outcomes.

Samples ID	Crack-load. (kN)	Service moment $-0.3M_p$ (kN.m)	Post-cracking rigidity (kN/mm)	Peak-load. (kN)	Displacement @ Peak load (mm)	Peak moment M_a(kN.m)	Strain energy (N-mm)	Deformation factor (DF) mm
GFRC 00	20	6.72	10	64	11	22.4	56776	0.8
GFRC 2.5	30	9.56	16.7	91	6.9	31.9	118231	1.13
GFRC 4.0	30	10.71	25	102	8.5	35.7	149600	1.32
GFRC 5.5	30	13.2	28.6	124	23	44	226352	1.6
RC 00	30	12.4	33	118	26.5	41.3	193008	1.4
RC 2.5	40	12.81	37	122	13	42.7	212505	1.52
RC 4.0	40	13.2	38.5	124	6.5	41.3	221093	1.64
RC 5.5	40	13.86	40	132	10.5	46.2	256500	1.7

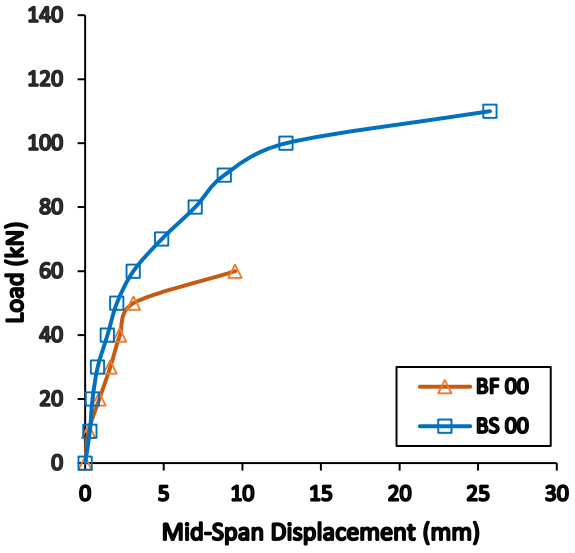

a. Comparison between steel and GFRP beams with no PO fiber.

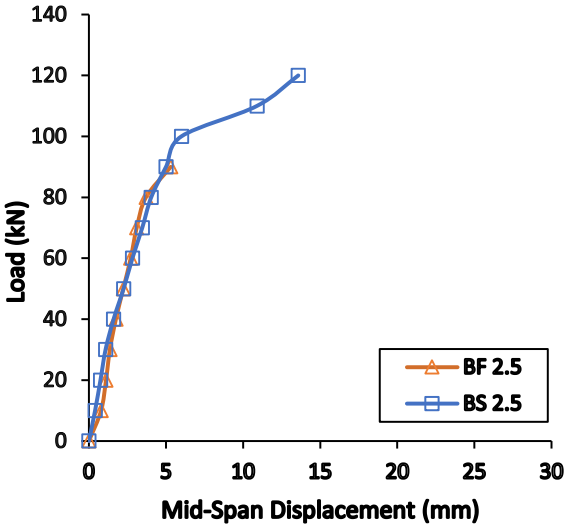

b. Comparison between steel and GFRP beams with PO fiber ratio 0.28%.

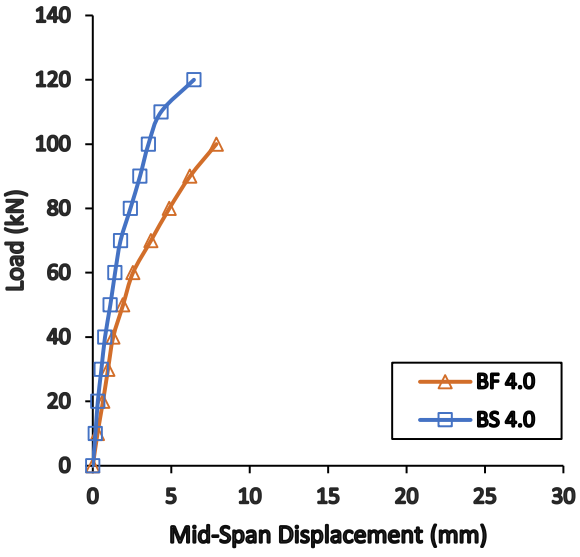

c. Comparison between steel and GFRP beams with PO fiber ratio 0.44%.

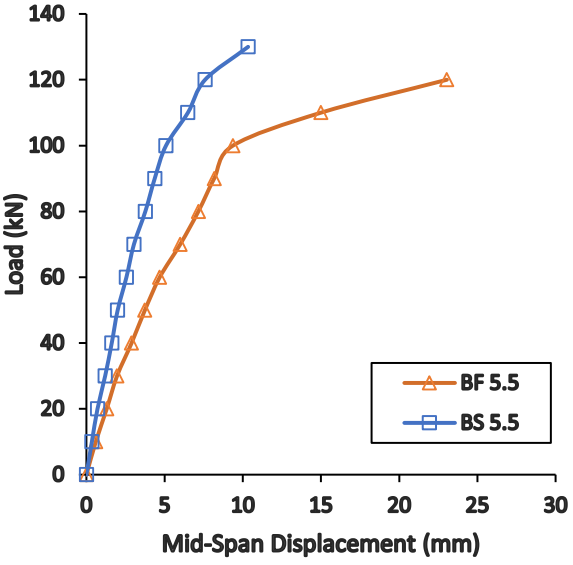

d. Comparison between steel and GFRP beams with PO fiber ratio 0.6%.

Fig. 10. Comparison between steel and GERP beams with different PO fiber ratio.

produced post-cracking rigidity improvement in comparison to control beams with no fibers. That could be as a result of restrictions on the width of the crack, which decreased the pullout of fiber. The average peak load of (RC 2.5) beam was discovered to be 122 kN, which had a slight increase about beam (RC 00) that was 118 kN. The ultimate displacement of the (RC 0.25) beams was 13 mm,

which was just 49% of steel-reinforced control beam. When compared to (RC 00) specimen, the incorporation of 0.28% fiber enhanced the deformation factor and strain energy loss by 0.08% and 0.1% consequently, for beams with (RC 2.5). The fiber's role in fracture arresting caused the pseudo-ductility or enhanced deformation factor, which caused tensile stresses to be transferred across the cracked planes. Additionally, the presence of fibers raised the concrete's ultimate failure strain in the compression, that consequently increased deformation factor.

5.1.4. GFRP and steel reinforced beams using 0.44% fiber

The incorporation of 0.44% macro synthetic fibers to reinforced GFRP samples improved post-cracking stiffness and reduced load drop after cracking; the load reduction following the initial crack decreased from 30 to 20 kN. Furthermore, in comparison to the beams with no fibers (GFRC 00), the post-cracking rigidity rose by 60%. The peak load of (GFRC 4.0) increased by 60% when compared to the control beam (GFRC 00), and the deformation factor increased by 0.65%.

For steel reinforced beam (RC 4.0), In comparison to control specimens (RC 00), The inclusion of 0.44% fibers contributed to an increase in the post-cracking rigidity by 17% (38.5 kN/mm), and the peak load increased by 5%. In addition, the mode of failure shifted from under steel reinforcement yielding to over-reinforced compression failure in flexure mode in comparison to (RC 00) specimen; the deformation factor and strain energy of steel-reinforced specimen (RC 4.0) was improved by 0.17% and 0.15%, respectively, with the addition of 0.4% synthetic fibers. The failure displacement has also decreased since the amount of fiber consumed has increased for steel reinforced specimens. The primary cause of the rise in the deformation factor was the inclusion of fibers, which increased the final strain of the concrete under compression.

5.1.5. GFRP and steel reinforced beams using 0.6% fiber

The incorporation of 0.6% high fiber volume to GFRP reinforced beams (GFRC 5.5) improved post-crack rigidity with 86% contrasted with beams devoid of fibers (GFRC 00). Additionally, a 0.6% fiber addition resulted in a considerable reduction of the load drop after cracking from 30 to 20 kN. The specimens improved just slightly at peak load. Decreased width of crack and deflections at high fiber doses in low FRP reinforced samples were the cause of the improved deformation factor.

For the steel reinforcement beam (RC 5.5), The post-crack rigidity enhanced with 0.6% fibers, nearly 22%. In comparison to samples that have low fiber dose, beams that had 1.0% fiber dose showed an increased peak load. Previous research revealed similar results (Yoo et al., 2016b; Patil et al., 2020; Ruan et al., 2020). Where the enhanced peak strength with high fiber doses decreases because of factors similar as fiber unbalanced distribution and balling. The inclusion of 0.6% fiber raised the factor of deformation by 1% at GFRP beam and 0.25% at the steel beam.

5.2. Crack patterns and mode of failure

According to Figs. 11 and 12, The cracking behavior of all tested beams is recorded at several loading stages during the flexural test, including the beginning of the first crack, the service load, and the ultimate load. The initial stage and the development of any beam cracks is determined by the mechanical qualities of the materials used, mainly the concrete mix's tensile strength and the type of reinforcing. The crack patterns of all beams. The failure mode of beams reinforced with steel was a standard under-reinforced flexure mode (For example, steel yields way under tension, then concrete collapses with compression). The crack of failure first appeared in the zone of constant moment and grew wider as the imposed load increased. When substituting steel with GFRP bars of identical area, the beams collapsed in a rapid brittle appearance as a result of FRP bar rupture in tension without deformation features. The beams failed abruptly brittle due to a tension related FRP bar rupture with no deformability features after replacing steel with the same area GFRP bars. The insertion of 0.28% PO fibers into GFRP reinforced beam had no effect on the flexural compression failure mode because a modest dosage of PO fibers did not considerably enhance the maximum strain of material (Lakavath et al., 2022). With increasing in the percentage of PO fibers in concrete beams, the deformation factor was increased because fiber contributes to improving the final concrete's compression-induced strain. When steel was substituted by GFRP bars of equal area, the pattern of failure changed from flexure to shear-flexure. Fig. 13 illustrates the general shape of load-deflection curve, the load-deflection curve for first cracks and finally crack characterizations.

The observed modes of failure for the tested beams can be classified into three types. The first was the tension failure known as ductile flexural failure mode (For example, bars yield way under tension, then concrete collapses with compression) in beams GFRC 2.5, GFRC 4.0, and RC 00. The

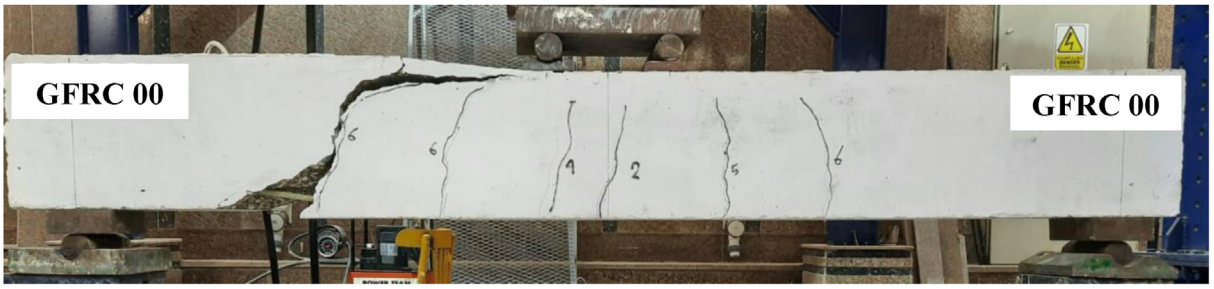

Note: 'GFRC 00' Fiber reinforced beam with PO fiber volume 00

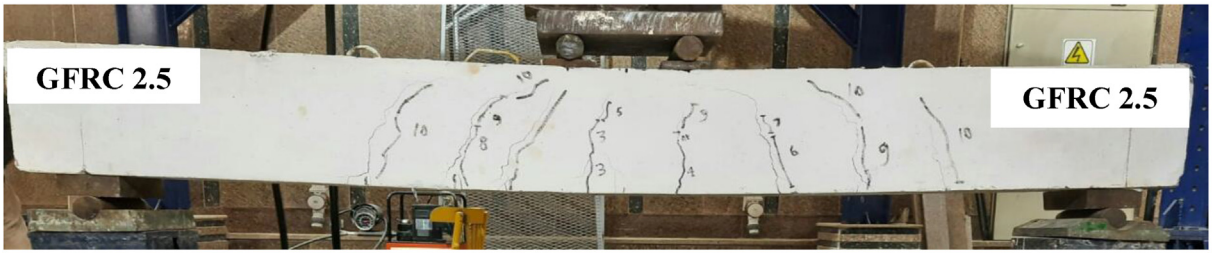

Note: 'GFRC 2.5' Fiber reinforced beam with PO fiber volume 2.5 kg/m^3

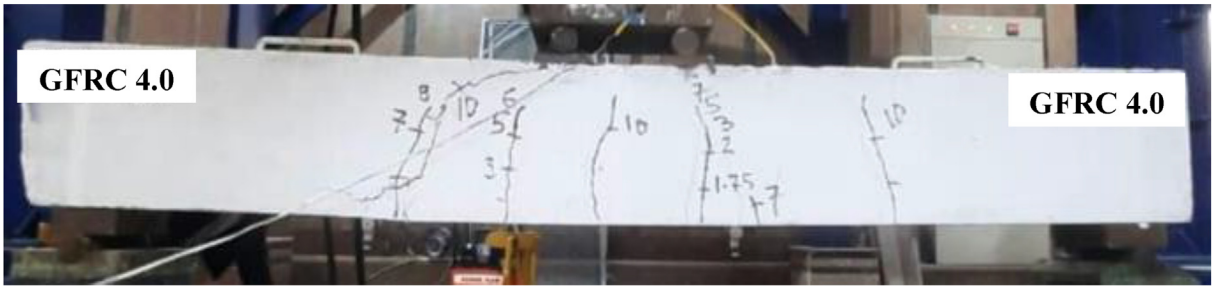

Note: 'GFRC 4.0' Fiber reinforced beam with PO fiber volume 4.0 kg/m^3

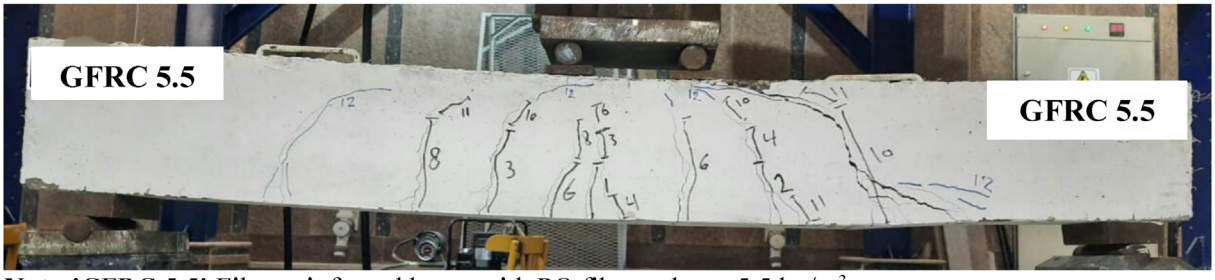

Note: 'GFRC 5.5' Fiber reinforced beam with PO fiber volume 5.5 kg/m^3

Fig. 11. Crack patterns and failure modes for HSC beams reinforced with GFRP bars.

second was a flexural failure accompanied by one large shear crack, which appeared only in beam GFRC 00. The third was flexural failure accompanied by local top crushing, which was seen in beams GFRC 5.5, RC 2.5, RC 4.0, and RC 5.5 as shown in Figs. 11 and 12. The first cracks appeared in beams GFRC 00 and RC 00, which had no internal fibers, at loads of 20 and 30 kN, respectively. These measured cracking loads were approximately 31.25% and 25.42% of the ultimate loads 'Peak-load' of the beams GFRC 00 and RC 00, respectively. The detected cracks were at loads of 30 and 40 kN, respectively, for beams GFRC 2.5 and RC 2.5, which had polypropylene internal fibers with volume 2.5 kg/m^3 in their concrete mix. About 32.97% and 32.77% of the beams' GFRC 2.5 and RC 2.5 ultimate loads, respectively, were represented by these measured cracking loads.

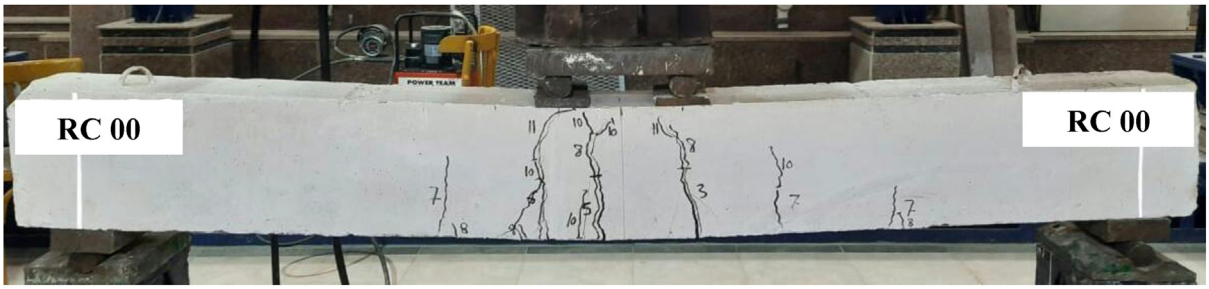

Note:'RC 00' Steel reinforced beam with PO fiber volume 0

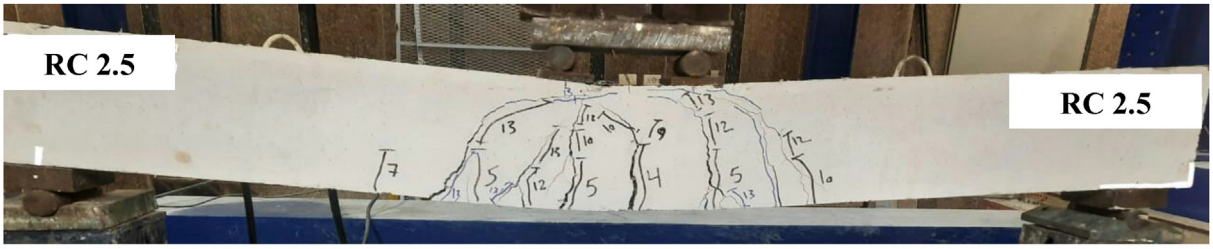

Note:'RC 2.5' Steel reinforced beam with PO fiber volume 2.5 kg/m^3

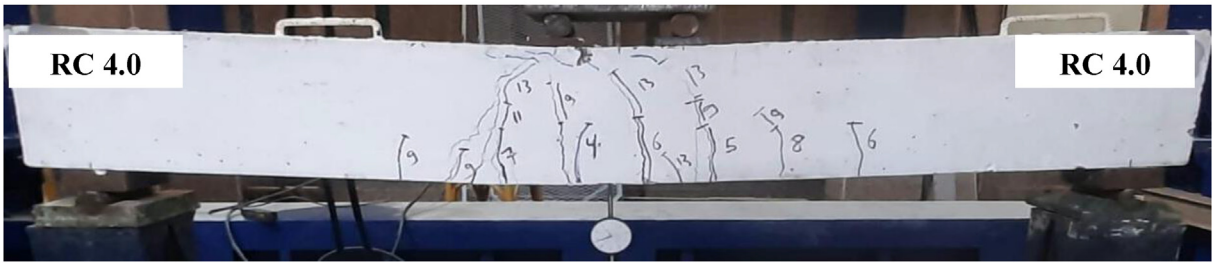

Note:'RC 4.0' Steel reinforced beam with PO fiber volume 4.0 kg/m^3

Note:'RC 5.5' Steel reinforced beam with PO fiber volume 5.5 kg/m^3

Fig. 12. Crack patterns and failure modes for HSC beams reinforced with steel bars.

For beams GFRC 4.0 and RC 4.0, which had polypropylene internal fibers with volume 4.0 kg/m^3 in their concrete mix, the first cracks were at loads of 30 and 40 kN, respectively. About 29.41% and 32.25% of the beams' GFRC 4.0 and RC 4.0 ultimate loads, respectively, were represented by these measured cracking loads. For beams GFRC 5.5 and RC 5.5, which had polypropylene internal fibers with volume 5.5 kg/m^3 in their concrete mix, the first cracks were at loads of 30 and 40 kN, respectively. About 24.19% and 30.30% of the beams' GFRC 5.5 and RC 5.5 ultimate loads, respectively, were represented by these measured cracking loads. From previously noted that the cracking load of beams

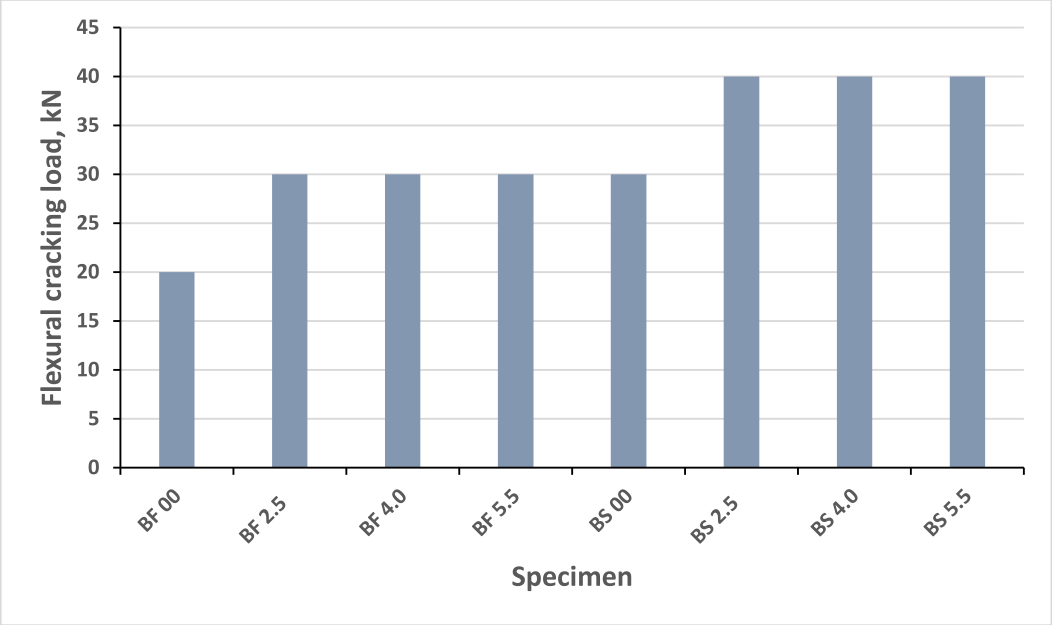

(a) First cracking load of all tested beams

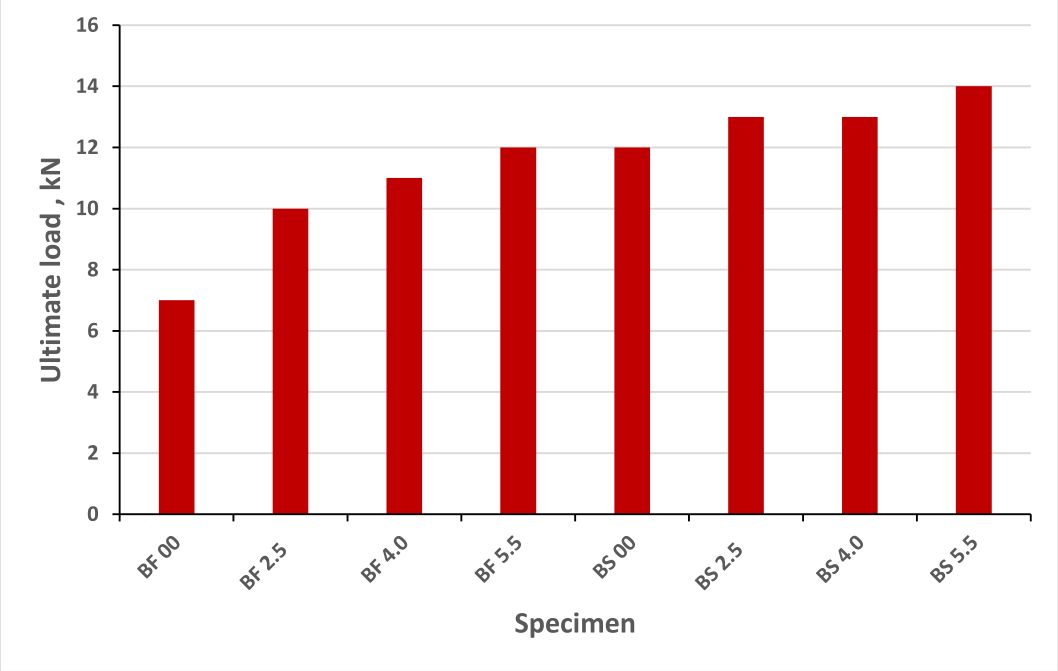

(b) Ultimate load of all tested beams

Fig. 13. First cracking and ultimate loads.

GFRC 00 and RC 00 are less than other beams. This is owing to the insertion of macro-synthetic fiber in concrete matrix which reduces cracks in concrete and raises the upper concrete strain to the ultimate load. The insertion of 0.25% PO fibers to GFRP reinforced beam had no effect on the flexural compression failure mode because a modest dosage of PO fibers did not considerably enhance the

maximum strain of material. With increasing in the percentage of PO fibers in concrete beams, the deformation factor was increased because fiber contributes to improving the final concrete's compression-induced strain. When steel was substituted by GFRP bars of equal area, the pattern of failure changed flexure to shear-flexure.

5.3. Behavior of GERP bars' load-strain

Fig. 14 illustrates a load-strain curve of the bottom GFRP bar's measured strain. It is evident the strain placed on the GFRP reinforcement grows linearly before the crack. After cracking, the GFRP bar's levels of strain significantly increased when the applied load was increased. The strain gauges' placements were in the middle of GFRP bottom bars. Table 10 shows the strain of GFRP bottom bars differs from 0.00466 to 0.008, note that the strain value was increased gradually with an increasing ratio of PO fiber. Therefore, the increased concrete's failure strain in compression prior to failure allows GFRP bars to be extended to greater strains as a result of fiber addition and avoids brittle failure caused by GFRP bar rupture. When fiber doses are high, strain levels are decreased as a result of the fibers' ability to stop cracks from forming and effectively redistribute the load. The maximum failure strain of GFRP bars was around 8002 micro strains. The comparison between the strain values of the bottom bar strain of the beam that's concrete mix contained no fibers, and the one that contained the maximum value of (0.6%) of fiber was 72%. The ultimate bottom bar strain on beams with steel bars had a consistent value of 0.006704 for four beams with various PO fiber ratios. As a result, GFRP bars recorded an increase of 63% in strain value compared to the bar strains of steel bars, this result agreed with that of Chellapandian et al. (2020).

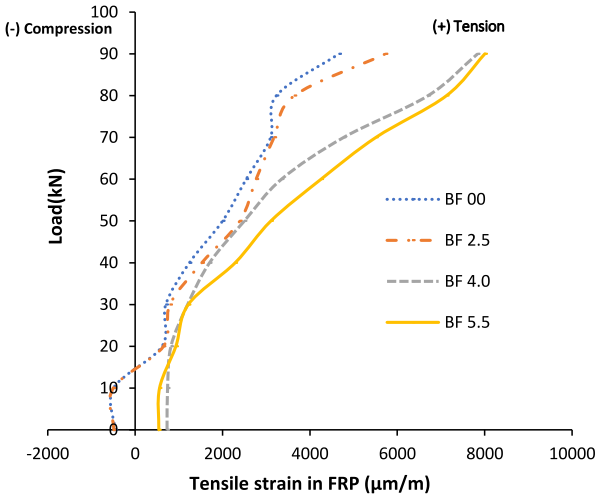

Fig. 14. Load-strain comparison of GFRP beams with different PO fibers.

6. Analytical analysis

6.1. Deflection calculations

Because FRP bars have a lower elastic modulus than steel reinforcing, the design of FRP- reinforced concrete members is often dictated by serviceability specifications. As a result, the FRP reinforced deflection calculations for members might differ from those for RC members using steel reinforcing. The ultimate load deflection limits were estimated for the FRP and steel RC members utilizing three current models from the literature. The various models taken for consideration in this research include (i) the model proposed in ACI 440.1R (ACI 440.1R-15, 2015; Adam et al., 2015) and (ii) The model proposed in ISIS 2007 (ISIS Canada Research Network (The Canadian Network of Centers of Excellence on Intelligent Sensing for Innovative Structures), 2001), (iii) The model proposed in Benmokrane et al. (Benmokrane and Masmoudi, 1996). Eq. (2) gives the four-point bending structure's elastic deflection equation for beams. The remaining parameters can be computed using Eqs. (3)–(5).

$$\Delta = \frac{PS}{48E_cI_e}\left(3L^2 - 4S^2\right) \tag{2}$$

$$I_g = \frac{b\,h^3}{12} \tag{3}$$

$$I_{cr} = \frac{b}{3}d^3k^3 + n_fA_fd^2(1-k)^2 \tag{4}$$

$$k = \sqrt{\left(\rho n_f\right)^2 + 2\rho n_f} - \rho n_f \tag{5}$$

6.1.1. Deflection as per ACI 440.IR-15

The effective moment of inertia (I_e) under flexure for FRP-reinforced RC members was calculated using an equation in ACI 440.IR (ACI 440.1R-15, 2015). The equivalent change is introduced as a factor "β_d" that explains internal reinforcement using FRP (Eq. (7)).

$$I_e = \left(\frac{M_{cr}}{M_a}\right)^3\beta_dI_g + \left[1 - \left(\frac{M_{cr}}{M_a}\right)^3\right]I_{cr} \le I_g \text{ where } M_a \ge M_{cr} \tag{6}$$

Where:

$$\beta_d = 0.2 \times \left(\frac{\rho_f}{\rho_{fb}}\right) \leq 1.0 \tag{7}$$

$$M_{cr} = \frac{F_{ctr} \times I_g}{y_t} \tag{8}$$

6.1.2. Deflection as per ISIS 2007

ISIS (ISIS Canada Research Network (The Canadian Network of Centers of Excellence on Intelligent Sensing for Innovative Structures), 2001) states that the employed equation to determine the effective moment of inertia (Ie) for FRP reinforced RC elements was provided in (Eq (9)). The deflection of the FRP-reinforced part is determined using Eq. (2), which contains a γ factor of 0.5 to extend the deflection response horizontally just after the crack.

$$I_e = \frac{I_g I_{cr}}{I_{cr} + \left(1 - 0.5\left(\frac{M_{cr}}{M_a}\right)^2\right)(I_g - I_{cr})} \tag{9}$$

6.1.3. Deflection in accordance with Benmokrane et al

Benmokrane et al. (Benmokrane and Masmoudi, 1996) and Yost et al. (2003) employ methods for reducing the gross and cracked moments of inertia by adding coefficients to Branson's equation, overestimating the deflection regards since the trials won't reveal the horizontal shift that their formulation produced. The equation is employed to determine the effective moment of inertia (Ie) provided in (Eq (10)).

$$I_e = xI_{cr} + \left(\frac{I_g}{\beta} - xI_{cr}\right)\left(\frac{M_{cr}}{M_a}\right)^3 \tag{10}$$

Where $x = 0.84$; $\beta = 7$.

The experimental results and the predictions derived from the various equations are contrasted and presented in Table 11. In comparison to the test findings, it was evident that each model overestimated the values of deflection and was moderate. Table 11 confirms the application of the recommended deflection equation indicated by three previous methods; the values of FRP beam's deflection were higher than the deflection's value of the test. The variation was observed to be greater as the dose of discrete PO fibers was increased. Disregarding the role that fiber plays in the mechanism for crack arrest resulted in a significant divergence from the test results.

7. Summary and conclusion

The purpose of this study was to measure the effect of varying macro-synthetic fiber volumes inclusion in the performing and behavior of GFRP and steel reinforced under flexure of concrete beams, eight geometrically equivalent large-scale beam specimens with GFRP and Steel as internal reinforcements without stirrups were put to the test under gradually increasing monotonic stress. Polypropylene fibers with a volume percentage of 0.28%,0.44% and 0.6% were included in the test samples' concrete mixture. A modified equation for GFRP beams is provided to estimate deflections at serviceability limits. The subsequent significant implications are possibly derived from the study's findings:

- The addition of PO fiber (0.6%) to the concrete mix slightly reduced compressive strength by 5%, while the split tensile strength was increased by 19% compared to normal concrete.
- The addition of synthetic fibers by 0.6% increased the residual flexural strengths of concrete specimens by 18.3% and improved the post-peak performance and ductility of concrete.
- Along with the volume ratio of polypropylene fiber increasing, In FRP and steel RC beams, the deflection and crack width were reduced, but the service load and ultimate load was higher.
- The use of macro-synthetic fibers greatly enhanced the post-crack rigidity of beams. The post-cracking stiffness increase ranged from 10 to 29 (kN/mm) for GFRP RC beams and varied

Table 10. Ultimate loads and strains of GFRP bars.

Specimen ID	Cross sec. dim.(mm)		Type of internal reinforcement	As (bott.)	Ultimate Load (kN)	Ultimate Bottom strain of bars ($\varepsilon_u \times 10^{-6}$)
	b	t				
GFRC 00	150	250	GFRP	2Ø10	64	4662.527
GFRC 0.25	150	250	GFRP	2Ø10	91	5729.629
GFRC 0.4	150	250	GFRP	2Ø10	102	7836.249
GFRC 0.55	150	250	GFRP	2Ø10	124	8002.235
RC 00	150	250	Steel	2Ø10	118	6704.327
RC 0.25	150	250	Steel	2Ø10	122	6704.327
RC 04	150	250	Steel	2Ø10	124	6704.327
RC 0.55	150	250	Steel	2Ø10	132	6704.327

Table 11. Limitations for the deflection of fiber-reinforced polymer (FRP) reinforced RC beams.

Specimen ID	Deflection limits as test result (mm)	Deflection limits as per ACI 440.IR-15 (mm)	Deflection limits as per ISIS 2007 (mm)	Deflection limits as per Benmokrane et al. (mm)
GFRC 00	11	14.64	18	19.6
GFRC 0.25	6.9	24.18	25.8	30
GFRC 0.4	8.5	28.36	30	35.8
GFRC 0.55	23	36	36.6	43.5
RC 00	26.5	9	8.12	9.82
RC 0.55	13	8.46	8.4	10.2
RC 0.4	6.5	8.67	8.59	10.4
RC 0.55	10.5	9.3	9.22	11.06

from 33 to 40 (kN/mm) for Steel reinforced beams using fiber doses that ranged from 0.0 to 0.55%.

- Macro-synthetic fibers provide great shear strength and can substitute transverse reinforcement in slender beams.
- Macro-synthetic fibers can transform brittle mode of failure into ductile ones.

8. Recommendation for future design

Based on the conclusions of this present study, the subsequent recommendations could be presented for future research work:

1- The influence of higher percentages of polypropylene fiber needs to be studied.
2- Other types of macro-synthetic fibers can be investigated in the production of GFRP concrete beams.
3- The experimental work done should be modeled with the help of finite element software.

Author contribution/author credit statement

Maryam M. Koura, Ahmed M. Tahwia and Mohamed H. Matthana contributed equally to this work. All authors have read and agreed to the published version of the manuscript.

Conflicts of interest

There are no conflict of interest.

References

Abdelkarim, O.I., Ahmed, E.A., Mohamed, H.M., Benmokrane, B., 2019. Flexural strength and serviceability evaluation of concrete beams reinforced with deformed GFRP bars. Eng. Struct. 186, 282–296.

ACI 440.1R-15, 2015. Guide for the Design and Construction of Structural Concrete Reinforced with FRP Bars. American Concrete Institute, Farmington Hills, MI, USA.

Adam, M.A., Said, M., Mahmoud, A.A., Shanour, A.S., 2015. Analytical and experimental flexural behavior of concrete beams reinforced with glass fiber reinforced polymers bars. Construct. Build. Mater. 84, 354–366.

Al-Enezi, M.S., Yousef, A.M., Tahwia, A.M., 2023. Shear capacity of UHPFRC deep beams with web openings. Case Stud. Constr. Mater. 18, e02105. https://doi.org/10.1016/j.cscm.2023.e02105.

Ashour, S.A., Hasanain, G.S., Wafa, F.F., 1992. Shear behavior of high-strength fiber reinforced concrete beams. Struct. J. 89, 176–184.

ASTM C293/C293M, 2016. Standard Test Method for Flexural Strength of Concrete (Using Simple Beam with Center-point Loading). ASTM International, West Conshohocken, PA, USA.

ASTM C469/C469M, 2014. Standard Test Method for Static Modulus of Elasticity and Poisson's Ratio of Concrete in Compression. ASTM International, West Conshohocken, PA, USA.

ASTM C496/C496M, 2017. Standard Test Method for Splitting Tensile Strength of Cylindrical Concrete Specimens. ASTM International, West Conshohocken, PA, USA.

Benmokrane, B., Masmoudi, R., 1996. Flexural response of concrete beams reinforced with FRP reinforcing bars. Structural J. 93 (1), 46–55.

BS EN 12390-3, 2009. Testing Hardened Concrete: Compressive Strength of Test Specimens. BSI, London, UK.

Buratti, N., Mazzotti, C., Savoia, M., 2011. Post-cracking behaviour of steel and macro-synthetic fibre-reinforced concretes. Construct. Build. Mater. 25 (5), 2713–2722.

Chellapandian, M., Mani, A., Prakash, S.S., 2020. Effect of macro-synthetic structural fibers on the flexural behavior of concrete beams reinforced with different ratios of GFRP bars. Compos. Struct. 254, 112790.

Dashti, J., Nematzadeh, M., 2020. Flexural behavior of GFRP bar-reinforced calcium aluminate cement concrete beams containing forta-ferro fibers in acidic environment. Construct. Build. Mater. 265, 120602.

Ding, Y., You, Z., Jalali, S., 2011. The composite effect of steel fibres and stirrups on the shear behaviour of beams using self-consolidating concrete. Eng. Struct. 33, 107–117. https://doi.org/10.1016/j.engstruct.2010.09.023.

El-Sayed, T.A., Algash, Y.A., 2021. Flexural behavior of ultra-high performance geopolymer RC beams reinforced with GFRP bars. Case Stud. Constr. Mater. 15, e00604.

El-Sayed, T.A., Erfan, A.M., Abdelnaby, R.M., Soliman, M.K., 2022. Flexural behavior of HSC beams reinforced by hybrid GFRP bars with steel wires. Case Stud. Constr. Mater. 16, e01054.

El-Sayed, T.A., Abdallah, K.S., Ahmed, H.E., El-Afandy, T.H., 2023. Structural behavior of ultra-high strength concrete columns reinforced with basalt bars under axial loading. Int. J. Concr. Struct. Mater. 17 (1), 43.

Erfan, A.M., Algash, Y.A., El-Sayed, T.A., 2019. Experimental & analytical flexural behavior of concrete beams reinforced with basalt fiber reinforced polymers bars. Int. J. Sci. Eng. Res. 10 (8), 297–315.

Erfan, A.M., Abd Elnaby, R.M., Badr, A.A., El-sayed, T.A., 2021. Flexural behavior of HSC one-way slabs reinforced with basalt FRP bars. Case Stud. Constr. Mater. 14, e00513.
Ge, W., Zhang, J., Cao, D., Tu, Y., 2015. Flexural behaviors of hybrid concrete beams reinforced with BFRP bars and steel bars. Construct. Build. Mater. 87, 28–37.
Imam, A., Tahwia, A., Elagamy, A., Yousef, M., 2021. Behavior of reinforced concrete beams strengthened with carbon fiber strips. Mansoura Eng. J. MEJ 29 (3), 22–40. https://doi.org/10.21608/bfemu.2021.140069.
ISIS Canada Research Network (The Canadian Network of Centers of Excellence on Intelligent Sensing for Innovative Structures), 2001. Reinforced concrete structures with fiber reinforced polymers. ISIS Manual no. 3.
Issa, M.S., Metwally, I.M., Elzeiny, S.M., 2011. Influence of fibers on flexural behavior and ductility of concrete beams reinforced with GFRP rebars. Eng. Struct. 33 (5), 1754–1763.
Joshi, S.S., Thammishetti, N., Prakash, S.S., 2018. Efficiency of steel and macro-synthetic structural fibers on the flexure-shear behavior of prestressed concrete beams. Eng. Struct. 171, 47–55.
Lakavath, C., Joshi, S.S., Prakash, S.S., 2019a. Investigation of the effect of steel fibers on the shear crack-opening and crack-slip behavior of prestressed concrete beams using digital image correlation. Eng. Struct. 193, 28–42.
Lakavath, C., Joshi, S.S., Prakash, S.S., 2019b. Investigation of the effect of steel fibers on the shear crack-opening and crack-slip behavior of prestressed concrete beams using digital image correlation. Eng. Struct. 193, 28–42.
Lakavath, C., Bhosale, A.B., Prakash, S.S., Sharma, A., 2022. Effectiveness of hybrid fibers on the fracture and shear behavior of prestressed concrete beams. Fibers 10 (3), 26.
Li, C., Zhu, H., Niu, G., Cheng, S., Gu, Z., Yang, L., 2022. Flexural behavior and a new model for flexural design of concrete beams hybridly reinforced by continuous FRP bars and discrete steel fibers. Structures 38, 949–960. Elsevier.
Liu, X., Sun, Y., Wu, T., 2019. Flexural capacity and deflection of fiber-reinforced lightweight aggregate concrete beams reinforced with GFRP bars. Sensors 19 (4), 873.
Nassif, M.K., Erfan, A.M., Fadel, O.T., El-sayed, T.A., 2021. Flexural behavior of high strength concrete deep beams reinforced with GFRP bars. Case Stud. Constr. Mater. 15, e00613.
Oudah, F., El-Hacha, R., 2012. A new ductility model of reinforced concrete beams strengthened using fiber reinforced polymer reinforcement. Compos. B Eng. 43 (8), 3338–3347.
Patil, G.M., Chellapandian, M., Prakash, S.S., 2020. Effectiveness of hybrid fibers on flexural behavior of concrete beams reinforced with glass fiber-reinforced polymer bars. ACI Struct. J. 117 (5).
Pereira, E.B., Fischer, G., Barros, J.A., 2012. Effect of hybrid fiber reinforcement on the cracking process in fiber reinforced cementitious composites. Cement Concr. Compos. 34 (10), 1114–1123.
Ruan, X., Lu, C., Xu, K., Xuan, G., Ni, M., 2020. Flexural behavior and serviceability of concrete beams hybrid-reinforced with GFRP bars and steel bars. Compos. Struct. 235, 111772.
Sahoo, D.R., Maran, K., Kumar, A., 2015. Effect of steel and synthetic fibers on shear strength of RC beams without shear stirrups. Construct. Build. Mater. 83, 150–158.
Sheikh, S.A., Kharal, Z., 2018. Replacement of steel with GFRP for sustainable reinforced concrete. Construct. Build. Mater. 160, 767–774.
Susetyo, J., Gauvreau, P., Vecchio, F.J., 2011. Effectiveness of steel fiber as minimum shear reinforcement. ACI Struct. J. 108, 488.
Tahwia, A.M., El-Far, O., Amin, M., 2022. Characteristics of sustainable high strength concrete incorporating eco-friendly materials. Innov. Infrastruct. Solut. 7 (1). https://doi.org/10.1007/s41062-021-00609-7.
Tahwia, A.M., Mokhles, M., Elemam, W.E., 2023a. Optimizing characteristics of high- performance concrete incorporating hybrid polypropylene fibers. Innov. Infrastruct. Solut. 8, 297. https://doi.org/10.1007/s41062-023-01268-6.
Tahwia, A.M., Helal, K.A., Youssf, O., 2023b. Chopped basalt fiber-reinforced high-performance concrete: an experimental and analytical study. J. Comps. Sci. 7 (6), 250.
Tran, T.T., Pham, T.M., Hao, H., 2020. Effect of hybrid fibers on shear behaviour of geopolymer concrete beams reinforced by basalt fiber reinforced polymer (BFRP) bars without stirrups. Compos. Struct. 243, 112236.
Wang, H., Belarbi, A., 2011. Ductility characteristics of fiber-reinforced-concrete beams reinforced with FRP rebars. Construct. Build. Mater. 25 (5), 2391–2401.
Yang, J.M., Min, K.H., Shin, H.O., Yoon, Y.S., 2012. Effect of steel and synthetic fibers on flexural behavior of high-strength concrete beams reinforced with FRP bars. Compos. B Eng. 43 (3), 1077–1086.
Yoo, D.Y., Banthia, N., Yoon, Y.S., 2016a. Predicting service deflection of ultra-high-performance fiber-reinforced concrete beams reinforced with GFRP bars. Compos. B Eng. 99, 381–397.
Yoo, D.Y., Banthia, N., Yoon, Y.S., 2016b. Predicting service deflection of ultra-high-performance fiber-reinforced concrete beams reinforced with GFRP bars. Compos. B Eng. 99, 381–397.
Yost, J.R., Gross, S.P., Dinehart, D.W., 2003. Effective moment of inertia for glass fiber-reinforced polymer-reinforced concrete beams. Struct. J. 100 (6), 732–739.
Yousef, A.M., Tahwia, A.M., Marami, N.A., 2018. Minimum shear reinforcement for ultra-high performance fiber reinforced concrete deep beams. Construct. Build. Mater. 184, 177–185. https://doi.org/10.1016/j.conbuildmat.2018.06.022.
Yousef, A.M., Tahwia, A.M., Al-Enezi, M.S., 2023. Experimental and numerical study of UHPFRC continuous deep beams with openings. Buildings 13, 1723. https://doi.org/10.3390/buildings13071723.
Zhu, H., Cheng, S., Gao, D., Neaz, S.M., Li, C., 2018. Flexural behavior of partially fiber-reinforced high-strength concrete beams reinforced with FRP bars. Construct. Build. Mater. 161, 587–597.